

# Photodissociation Dynamics of CH<sub>2</sub>ICl at 222, 236, 266, 280, and ~304 nm<sup>†</sup>

Dulal Senapati, K. Kavita, and Puspendu K. Das\*

Department of Inorganic and Physical Chemistry, Indian Institute of Science, Bangalore 560012, India

Received: April 26, 2002; In Final Form: May 31, 2002

Dynamics of I\*(<sup>2</sup>P<sub>1/2</sub>) formation from CH<sub>2</sub>ICl dissociation has been investigated at five different ultraviolet excitation wavelengths, e.g., 222, 236, 266, 280, and ~304 nm. The quantum yield of I\*(<sup>2</sup>P<sub>1/2</sub>) production,  $\phi^*$ , has been measured by monitoring nascent I(<sup>2</sup>P<sub>3/2</sub>) and I\* concentrations using a resonance enhanced multiphoton ionization detection scheme. The measured quantum yield as a function of excitation energy follows the same trend as that of methyl iodide except at 236 nm. The photodissociation dynamics of CH<sub>2</sub>ICl also involves three upper states similar to methyl iodide, and a qualitative correlation diagram has been constructed to account for the observed quantum yield. From the difference in behavior at 236 nm, it appears that the crossing region between the two excited states (<sup>3</sup>Q<sub>0</sub> and <sup>1</sup>Q<sub>1</sub>) is located near the exit valley away from the Franck Condon excitation region. The B- and C-band transitions do not participate in the dynamics, and the perturbation of the methyl iodide states due to Cl–I interaction is relatively weak at the photolysis wavelengths employed in this investigation.

## 1. Introduction

Photolysis studies on dihalomethanes are of importance in atmospheric and marine chemistry because the mono- and dihaloalkanes are the principal known source for active halogen atoms and radicals in the upper atmosphere and ocean water.<sup>1–2</sup> The haloalkanes dissociate by irradiation with UV light to produce active halogen atoms and radicals which play a major role in ozone depletion from the earth's ozone layer.

Photodissociation dynamics of alkyl halides in their A-band absorption in the near-ultraviolet has been extensively studied by both experiment<sup>3–5</sup> and theory<sup>6–9</sup> over the past three decades. In fact, the dynamics of CH<sub>3</sub>I dissociation has served as a model for understanding polyatomic fragmentation pattern in the gas phase. In contrast to iodomethane, very little has been done to investigate the A-band photodissociation of dihaloalkanes such as chloriodomethane (CH<sub>2</sub>ICl).<sup>10–12</sup> Apart from its role in the upper atmosphere destruction of ozone, in many ways, dihaloalkanes are interesting systems to probe the carbon–halogen bond-breaking process. First, the effect of geminal halogen substitution on the carbon halogen bond scission can be examined. Second, the mixed dihaloalkanes offer a large number of potential dissociation pathways, and by a proper choice of the excitation wavelength, a particular carbon halogen bond could be broken and thus bond selective photodissociation be achieved.

Here, we focus on the I\* (<sup>2</sup>P<sub>1/2</sub>) quantum yield measurement from the photolysis of chloriodomethane in the near-ultraviolet covering the entire A band centered on the C–I bond. The longest wavelength absorption in chloriodomethane peaks at 271 nm and covers the wavelength range 225–325 nm (called the A band). The band arises due to the transition of a nonbonding electron (n) of the iodine atom to an antibonding molecular orbital ( $\sigma^*$ ) localized on the C–I bond. This band is red-shifted with respect to the methyl iodide A band because the presence of the chlorine atom in chloriodomethane

stabilizes the  $\sigma^*$  (C–I) antibonding orbital more than the ground nonbonding orbital, n (I). In methyl iodide where the A-band absorption peaks at 258 nm, excitation around 258 nm is predominantly to the <sup>3</sup>Q<sub>0</sub> state which correlates to I\* product at the asymptotic limit. There are two other transitions that are possible within the A band. They are <sup>1</sup>Q<sub>1</sub> ← <sup>1</sup>A<sub>1</sub> and <sup>3</sup>Q<sub>1</sub> ← <sup>1</sup>A<sub>1</sub> transitions. Both the <sup>1</sup>Q<sub>1</sub> and the <sup>3</sup>Q<sub>1</sub> states correlate to the ground-state I (<sup>2</sup>P<sub>3/2</sub>) product. From angular anisotropy measurements<sup>13–17</sup> and I\* quantum yield measurement by various spectroscopic schemes,<sup>18–24</sup> the dynamics of methyl iodide photodissociation has been understood to a large extent. Near the maximum of the A-band absorption, the transition strength in CH<sub>3</sub>I is carried mostly by the parallel transition <sup>3</sup>Q<sub>0</sub> ← <sup>1</sup>A<sub>1</sub>, and any ground-state I atom at this wavelength is produced by the curve crossing mechanism between the <sup>3</sup>Q<sub>0</sub> and <sup>1</sup>Q<sub>1</sub> states. However, at excitation wavelengths in the red and blue wings of the A band, the involvement of the <sup>3</sup>Q<sub>1</sub> and <sup>1</sup>Q<sub>1</sub> states, respectively, play an important role in the dynamics.

In chloriodomethane, photoexcitation within the A band centered on the C–I bond should predominantly lead to the cleavage of the C–I bond, although the states involved in the dissociation will no longer have the same symmetry as those in CH<sub>3</sub>I. A second band localized on the C–I bond peaking at 192 nm and more intense than the A band, is also seen in CH<sub>2</sub>ICl (Figure 1a). This is the B band of chloriodomethane, and it arises from the excitation of a 5p<sub>π</sub> nonbonding electron on the iodine atom to the next Rydberg state (6s). Unlike the A band, this band is blue shifted with respect to that in methyl iodide by about 6 nm (the B-band maximum in CH<sub>3</sub>I is at 198 nm). This is due to the electron withdrawing effect of the chlorine atom on the C–I bond, which increases the molecular ionization potential followed by a shift in the Rydberg states. The next higher energy band, that is, the C band, in CH<sub>2</sub>ICl located in the vacuum ultraviolet originates from an n →  $\sigma^*$  transition localized on the C–Cl bond. The same band in CH<sub>3</sub>Cl shows an absorption maximum at 173 nm with spreading from 167 to 182 nm.<sup>25</sup> Because the presence of an iodine atom in CH<sub>2</sub>ICl is likely to stabilize the  $\sigma^*$  orbital to some extent,

<sup>†</sup> Part of the special issue "Donald Setser Festschrift".

\* To whom correspondence should be addressed.

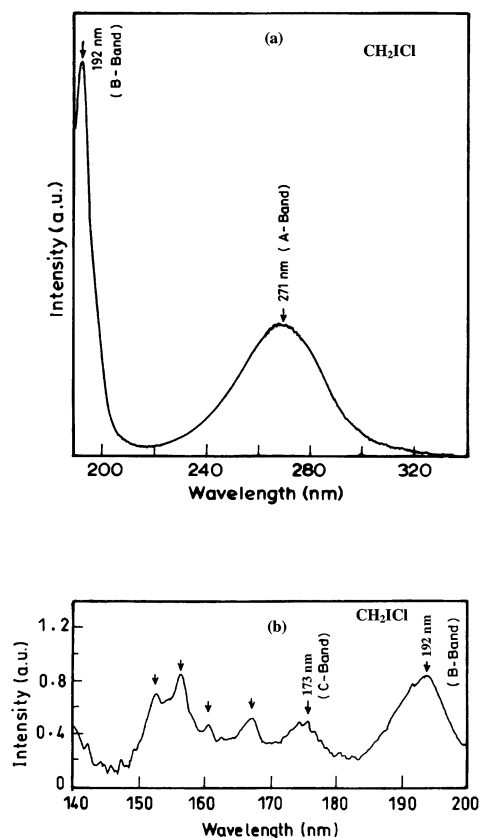


**Figure 1.** Gas-phase absorption spectra of  $\text{CH}_2\text{I}$ .

we expect this C–Cl band (C band) to shift to the red with respect to that in  $\text{CH}_3\text{I}$ . This band is expected to play a specific role in the photodissociation dynamics of  $\text{CH}_2\text{I}$  only below 200 nm.

In this paper, we report the  $\text{I}^*$  quantum yield from  $\text{CH}_2\text{I}$  at five different excitation wavelengths, viz., 222, 236, 266, 280, and  $\sim 304$  nm, in the gas phase covering the entire A band centered on the C–I chromophore. The resonance enhanced multiphoton ionization (REMPI) technique has been used to detect iodine fragments in the ground as well as excited states. The results have been discussed on the basis of what is known from alkyl iodide photodissociation studies. Some new insights into the photodissociation dynamics of mixed haloalkanes have also been provided.

## 2. Experimental Section

The experimental setup has been described in detail elsewhere.<sup>26</sup> In brief, the photodissociation experiments were carried out inside a stainless steel chamber evacuated continuously by a diffusion pump backed by a rotary pump to a base pressure of  $10^{-6}$  Torr. A constant sample pressure between 200 and 500  $\mu\text{Torr}$  was maintained throughout each experiment. The pump and probe laser beams were aligned perpendicular to each other at the center of the chamber between two electrodes ( $2.5 \times 2.5$  cm<sup>2</sup> and 0.5 mm thick stainless steel plates). The pump and probe laser wavelengths were generated by various frequency doubling and mixing schemes described earlier.<sup>27</sup> The probe beam was focused (ca. 0.01 cm dia) using a short focal length (5 cm fused silica) lens and the pump beam was contracted (0.5 cm dia) by a long focal length (typically 1 m f.l.) lens. The delay between the pump and probe lasers was maintained at  $\sim 200$  ns throughout each experiment. The iodine atoms in the ground and excited states produced in the photodissociation

**TABLE 1:  $\text{I}^*$  Quantum Yield ( $\phi^*$ ) from  $\text{CH}_2\text{I}$  at Different Photolysis Wavelengths**

pump wavelengths $\lambda$ (nm)	$\text{I}^*$ quantum yield ( $\phi^*$ )
222 nm	$0.47 \pm 0.02$
236 nm	$0.51 \pm 0.01$
266 nm	$0.51 \pm 0.02$
280 nm	$0.55 \pm 0.03$
304 nm	$0.38 \pm 0.01$

were detected by a REMPI scheme<sup>28</sup> known in the literature. Through one of the side ports of the vacuum chamber, a homemade REMPI detector with parallel plate electrodes, above and below the crossing point of the pump and probe laser beams, was placed. The anode was maintained at +100 V, and the voltage drop at the cathode across a 1 M $\Omega$ /1 W resistor to the ground was taken as signal. The output from the ion detector was collected through a homemade electrometer, amplified (typically 25 times), averaged over 50 shots in a gated boxcar (SRS 250), and displayed on a stripchart recorder. The pump laser polarization was kept unchanged because, in our experiments, atoms are detected and their recoil direction with the rotation of the pump laser polarization should not influence the REMPI signal intensity. Chloriodomethane and methyl iodide were purchased from Aldrich, USA and were fractionally distilled prior to each experiment. The gas-phase absorption spectrum of  $\text{CH}_2\text{I}$  in the ultraviolet was recorded in a Cary 210 spectrometer. The spectra in the vacuum ultraviolet was taken in a double beam assembled spectrometer where a  $\text{H}_2$  discharge was used as the light source, and the cell compartment of the spectrometer was maintained under high vacuum throughout the measurements.

## 3. Results and Discussion

The UV absorption of  $\text{CH}_2\text{I}$  in Figure 1a shows a broad peak with a maximum at 271 nm corresponding to the  $n \rightarrow \sigma^*$  transition localized on the C–I bond. This band is shifted to longer wavelengths by about 13 nm compared to that in  $\text{CH}_3\text{I}$  in which this band peaks at 258 nm. The gas-phase ultraviolet absorption spectrum is similar to what was seen earlier by Kwok et al.<sup>11</sup> A second broad band in  $\text{CH}_2\text{I}$  starts at 225 nm, grows much bigger than the A band, and peaks at 192 nm. This is assigned as the B band arising out of a Rydberg transition in the iodine atom. The C band originating from the  $n \rightarrow \sigma^*$  transition localized on the C–Cl bond is seen in Figure 1b. It peaks at  $\sim 173$  nm which is surprisingly the same as the position of the A-band maximum in  $\text{CH}_3\text{I}$ . The C band of  $\text{CH}_2\text{I}$  starts at 169 nm and extends up to 183 nm. This implies that the presence of the iodine atom does not affect the transitions originating from the C–Cl bond in chloriodomethane. In other words, the mixing of the iodine Rydberg states and the C–Cl antibonding state is rather weak. The other shorter wavelength bands seen in Figure 1b are due to Rydberg transitions localized either on the chlorine or iodine atoms.

The REMPI spectra from I and  $\text{I}^*$  were recorded by scanning the probe laser across the (2 + 1) ionization lines<sup>29</sup> of I (304.67 nm) and  $\text{I}^*$  (304.02 nm). The relative quantum yield of  $\text{I}^*$ ,  $\phi^* = \{N(\text{I}^*)\}/\{N(\text{I}) + N(\text{I}^*)\}$ , was determined directly from REMPI signal intensity and is listed in Table 1. The ratio of the measured REMPI signals from I [ $S(\text{I})$ ] and  $\text{I}^*$  [ $S(\text{I}^*)$ ] may be expressed as

$$\frac{N(\text{I})}{N(\text{I}^*)} = \frac{S(\text{I}) F(\text{I}) \sigma(\text{I}) \sigma(\text{RI})}{S(\text{I}^*) F(\text{I}^*) \sigma(\text{I}^*) \sigma^*(\text{RI})} \quad (1)$$

where  $\sigma^*(\text{RI})$  and  $\sigma(\text{RI})$  are the absorption cross sections of

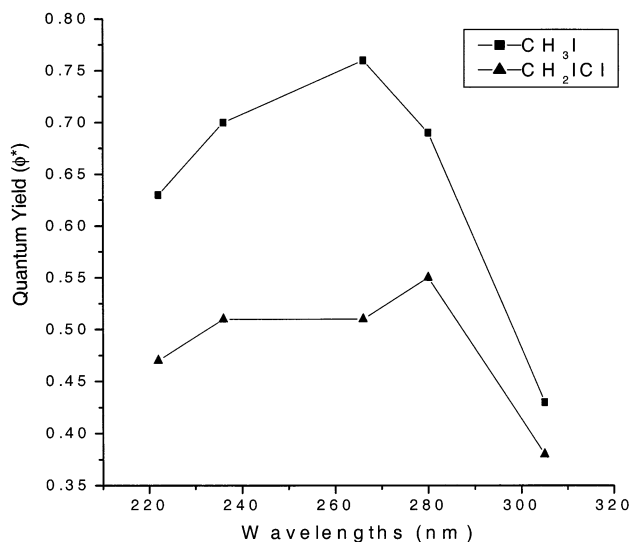


**Figure 2.** I\* quantum yield of CH<sub>3</sub>I and CH<sub>2</sub>ICI as a function of photolysis wavelength. The quantum yields for CH<sub>3</sub>I have been taken from refs 17, 26 (304 nm), 26 (280 nm), 15, 26 (266 nm), 34 (236 nm), and 35 (222 nm).

alkyl mono/dihalides at [2+1] REMPI wavelengths.  $N$  is the number density of the iodine atoms,  $F$  is the collection efficiency of the ion signals by the detector, and  $\sigma(I)$  and  $\sigma(I^*)$  are the REMPI cross-section of the ground and spin-orbit excited iodine atoms. As in the A-band absorption continuum, absorbance remains more or less constant in a narrow wavelength range (304.02–304.67 nm), and we take the ratio  $\{\sigma(RI)\}/\{\sigma^*(RI)\}$  as unity. We evaluated the ratio of the product of the REMPI cross section and collection efficiency of I\* and I, i.e.,  $[I^*]/[I]$ , as  $1.00 \pm 0.05$  using an I<sub>2</sub> photolysis study at 304.02 and 304.67 nm in our apparatus, which should yield equal amounts of I and I\*.<sup>30</sup> This value of  $1.00 \pm 0.05$  is close to the expected value and the value of 0.90 reported by Eppink et al.<sup>24</sup> Thus, we define a calibration factor, “ $k$ ”, as

$$\frac{N(I)}{N(I^*)} = k \frac{S(I)}{S(I^*)} \quad (2)$$

which we take as 1.0, and the quantum yields at various wavelengths were determined directly from the I\* and I signals.

The I\* quantum yield is maximum at 280 nm, and it decreases as we move to other excitation wavelengths on either side of the A-band maximum. The I\* yield from CH<sub>2</sub>ICI as a function of excitation wavelength has been shown in Figure 2. The observed variation of  $\phi^*$  with photolysis wavelength around the A-band maximum is similar to that observed in the case of methyl iodide except that the quantum yield in the latter is significantly higher at all wavelengths. This is opposite to what has been observed in fluorinated alkyl iodides. In trifluoromethyl iodide,  $\phi^*$  is higher than that in methyl iodide over the entire A band.<sup>27,31</sup> The quantum yield in CH<sub>2</sub>ICI peaks at 280 nm which is close to the absorption maximum, and the quantum yield decreases by 4% as we go to 266 nm or by 30% at 304 nm. At 236 nm, the quantum yield remains the same as that at 266 nm, and as the excitation wavelength is reduced further to 222 nm, the quantum yield drops slightly. The trend in quantum yield variation in chloriodomethane is similar to that in methyl iodide except a little difference at 236 nm. At 236 nm, the  $\phi^*$  in methyl iodide drops from that at 266 nm, whereas it remains unaltered in chloriodomethane. From all of these quantum yield results, we infer that the chloriodomethane dissociation follows a mechanism similar to that of methyl iodide dissociation over

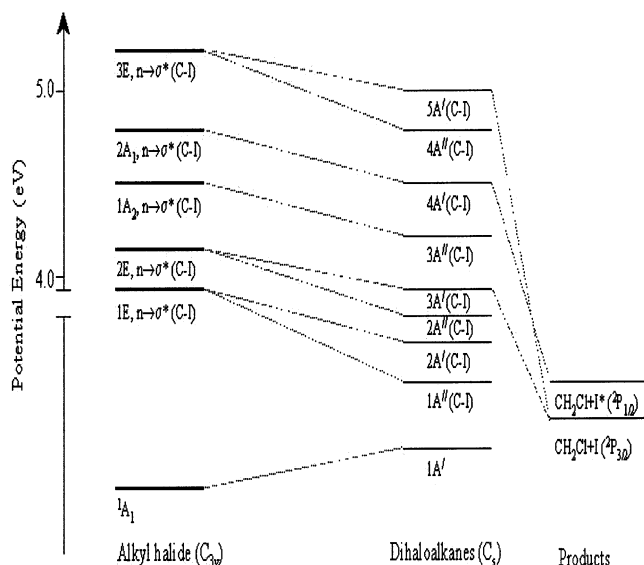


**Figure 3.** Schematic correlation diagram for the A-band transitions. The left-hand side shows the A-band transitions in CH<sub>3</sub>I. The relative energies for the various states have been taken from refs 25, 33, and 36. The states for CH<sub>2</sub>ICI are shown in the central column. Only the lowest four dissociation channels have been considered while constructing the diagram.

the entire A band, and the perturbation of the C–I antibonding state ( $\sigma^*$ ) by the presence of the electronegative chlorine atom is rather weak.

A schematic correlation diagram for chloriodomethane dissociation has been constructed (Figure 3). Only the low energy dissociation channels have been considered. On the left-hand side of the diagram, the A-band states of CH<sub>3</sub>I are displayed. This diagram explains how we can gain access to different potential energy surfaces at different excitation energies. At 280 nm, most of the transition strength in CH<sub>2</sub>ICI which has C<sub>s</sub> symmetry is carried by the 4A' state which is equivalent to the <sup>3</sup>Q<sub>0</sub> state of CH<sub>3</sub>I having C<sub>3v</sub> symmetry. The 4A' state correlates to I\* fragment. However, because of an avoided crossing with another state with the same symmetry, 5A', which is correlated to I, some amount of I is produced in the photolysis. At 266 nm, the mechanism is similar except that the curve crossing is more efficient, and the I\* yield decreases by ~4% from that at 280 nm. As we move to wavelengths longer than 280 nm, direct excitation to another state, 3A', which gives rise exclusively to I atoms, becomes possible. At ~304 nm, the contribution of the 3A' state to the total transition strength must be significant because we observe about 61% of the products as I atoms. Because the quantum yields at 266 and 236 nm are the same, the implication is that the actual potential energy surfaces with 4A' and 5A' symmetry cross near the exit channel and not close to the Franck–Condon region. For the ground-state chloriodomethane molecules, direct access to the 5A' state needs more photon energy, and perhaps, this is fulfilled to a small extent at 222 nm where the quantum yield decreases slightly from 236 nm. The nature of the curve crossing between the 4A' and 5A' states in chloriodomethane cannot be described adequately in one dimension. If an one-dimensional potential description were true, a classical soft-radical Landau–Zener curve crossing model<sup>32</sup> would predict an increase in the I\* quantum yield as a function of wavelength. However, this is not found. In the simplistic Landau–Zener curve crossing model, the I\* quantum yield is expected to increase with increase in velocity at the crossing region. Because most of the available energy after breaking the C–I bond in alkyl iodides is known

to be disposed as product translation,<sup>33</sup> we would expect an increase in the velocity of the excited chloriodomethane molecules as they roll on the upper state surface as the excitation energy is increased. In other words, we do not see an increase in quantum yield as a function of excitation energy in chloriodomethane dissociation, and from, this we infer that the dynamics of dissociation of this molecule cannot be explained adequately by one-dimensional potential energy diagrams. This is also supported by short time photodissociation dynamics studies of Kwok et al.,<sup>11</sup> who looked at the short time resonance Raman spectra of this molecule after excitation. Along with the stretching of the C–I bond, some bending modes are excited in the molecule. Coupling of the bending modes with that of the C–I stretch will perhaps be necessary for describing the dynamics of dissociation. The B-band contribution to the total absorption cross section is likely to be negligible over the entire wavelength range which we have employed, since the B-band absorption starts only at 225 nm and peaks at 192 nm. We also think that the contribution of the C-band peaking at 173 nm and centered on the C–Cl chromophore is insignificant at all of the dissociation wavelengths employed here. In other words, at the wavelengths employed by us, the dissociation dynamics of CH<sub>2</sub>ICl remains confined to the A band.

**Acknowledgment.** It gives us great pleasure to dedicate this paper in honor of Prof. Donald Setser who, through his work and dedication in physical chemistry, has inspired generations of gas phase chemists. We are grateful to Jack Preses, Richard Holroyd, and Christopher Fockenber for recording the gas phase spectra of CH<sub>2</sub>ICl reported here. We thank the Department of Atomic Energy, Government of India for generous funding.

## References and Notes

- (1) Mossinger, J. C.; Shallcross, D. E.; Cox, R. A. *J. Chem. Soc. Faraday Trans.* **1998**, *94*, 1391.
- (2) Vogt, R.; Sander, R.; Glasow, R. V.; Crutzen, P. J. *J. Atmos. Chem.* **1999**, *32*, 375.
- (3) Phillips, D. L. *Prog. React. Kinet. Mech.* **1999**, *24*, 223.
- (4) Matsumi, Y.; Tonokura, K.; Kawasaki, M.; Inoue, G.; Satyapal, S.; and Bersohn, R. *J. Chem. Phys.* **1991**, *94*, 2669.
- (5) Van Veen, G. N. A.; Baller, T.; de Vries, A. E. *Chem. Phys.* **1985**, *92*, 59.
- (6) Amatatsu, Y.; Yabushita, S.; Morokuma, K. *J. Chem. Phys.* **1996**, *104*, 9783.
- (7) Hammerich, D. A.; Manthe, U.; Kosloff, R.; Meyer, H. D.; Cederbaum, L. S. *J. Chem. Phys.* **1994**, *101*, 5623.
- (8) Tedjeddine, M.; Flament, J. P.; Teichteil, C. *Chem. Phys.* **1987**, *118*, 45.
- (9) Guo, H.; Schatz, G. C. *J. Chem. Phys.* **1990**, *93*, 393.
- (10) Kwok, W. M.; Phillips, D. L. *Chem. Phys. Lett.* **1997**, *270*, 506.
- (11) Kwok, W. M.; Phillips, D. L. *Mol. Phys.* **1997**, *90*, 315.
- (12) Schmitt, G.; Comes, F. J. *J. Photochem. Photobiol. A: Chem.* **1987**, *41*, 13.
- (13) Furlan, A.; Gejo, T.; Huber, R. J. *J. Phys. Chem.* **1996**, *100*, 7956.
- (14) Kang, W. K.; Jung, K. W.; Kim, D. C.; Jung, K. H. *J. Chem. Phys.* **1996**, *104*, 5815.
- (15) Riley, S. J.; Wilson, K. R. *Faraday Discuss. Chem. Soc.* **1972**, *53*, 132.
- (16) Person, M. D.; Kash, P. W.; Butler, L. J. *J. Chem. Phys.* **1991**, *94*, 2557.
- (17) Hertz, R. A.; Syage, J. A. *J. Chem. Phys.* **1994**, *100*, 9265.
- (18) Donohue, T.; Wiesenfeld, J. R. *J. Chem. Phys.* **1975**, *63*, 3130.
- (19) Baughcum, S. L.; Leone, S. R. *J. Chem. Phys.* **1980**, *72*, 6531.
- (20) Brewer, P.; Das, P.; Ondrey, G.; Bersohn, R. *J. Chem. Phys.* **1983**, *79*, 720.
- (21) Hess, W. P.; Kohler, S. J.; Haugen, H. K. Leone, S. R. *J. Chem. Phys.* **1986**, *84*, 2143.
- (22) Ogorzalek Loo, R.; Haerri, H. P.; Hall, G. E.; Houston, P. L. *J. Chem. Phys.* **1989**, *90*, 4222.
- (23) Syage, J. A.; Steadman, J. J. *J. Phys. Chem.* **1990**, *94*, 7343.
- (24) Eppink, A. T. J. B.; Parker, D. H. *J. Chem. Phys.* **1998**, *109*, 4758.
- (25) Raymonda, J. W.; Edwards, L. O.; Russel, B. R. *J. Am. Chem. Soc.* **1974**, *96*, 1708.
- (26) Uma, S.; Das, P. K. *Can. J. Chem.* **1994**, *72*, 865.
- (27) Kavita, K.; Das, P. K. *J. Phys. Chem. A* **2001**, *105*, 315.
- (28) Felps, S.; Hochmann, P.; Brint, P.; McGlynn, S. P. *J. Mol. Spectrosc.* **1976**, *59*, 355.
- (29) Gedanken, A.; Robin, M. B.; and Yafet, Y. *J. Chem. Phys.* **1982**, *76*, 4798.
- (30) Hwang, H. J.; El-Sayed, M. A. *J. Phys. Chem.* **1991**, *95*, 8044.
- (31) Kavita, K.; Das, P. K. *Chem. Phys. Lett.* **2001**, *338*, 118.
- (32) Godwin, F. G.; Gorry, P. A.; Hughes, P. M.; Raybone, D.; Watkinson, T. M.; Whitehead, J. C. *Chem. Phys. Lett.* **1987**, *135*, 163.
- (33) Van Veen, G. N. A.; Baller, T.; de Vries, A. E. *Chem. Phys.* **1985**, *97*, 179.
- (34) Kavita, K.; Das, P. K. submitted for publication to Current Science.
- (35) Uma, S.; Das, P. K. *Chem. Phys. Lett.* **1995**, *241*, 335.
- (36) Gedanken, A.; Rowe, M. D. *Chem. Phys. Lett.* **1975**, *34*, 39.